

## Meniscus formation in a capillary and role of contact line friction

Taras Andruk<sup>a</sup>, Daria Monaenkova<sup>a,b</sup>, Binyamin Rubin<sup>a</sup>, Wah-Keat Lee<sup>c</sup>, and Konstantin G. Kornev<sup>a</sup>

<sup>a</sup> Department of Materials Science and Engineering, Clemson University, SC, 29634, USA; kkornev@clemson.edu

<sup>b</sup> School of Physics, Georgia Institute of Technology, GA, 30332, USA

<sup>c</sup> Advanced Photon Source, Argonne National Laboratory, Argonne, IL 60439, USA

### Supplementary Material

#### X-ray imaging of meniscus nucleation.

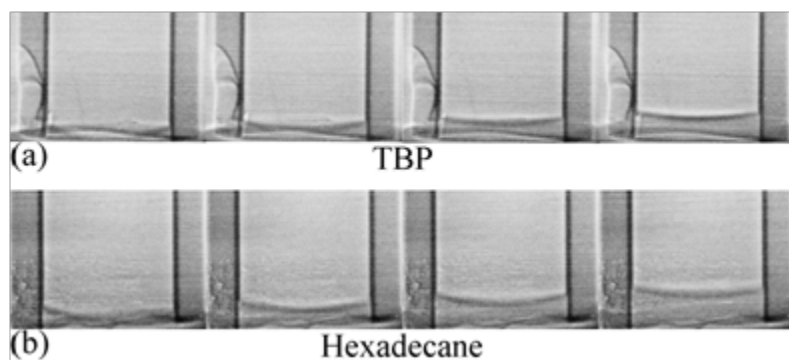


**Figure S1.** Nucleation of meniscus of a) TBP and b) hexadecane in a  $D_i = 400\mu\text{m}$  glass capillary. The frames are taken with the period of 1 ms.

**Contact angle determination.** Using the image analysis, we analyzed the equilibrium contact angles by studying the maximum column height given by Jurin's formula. The meniscus position was defined through its lower point, see the red dot in **Figure S2 b)**. To measure the height of the liquid column, two characteristic points were used. The zero – level of the liquid column was set at the free liquid surface far away from the capillary and the upper point was chosen at the meniscus sag. In parallel, we used the circular arc fit to obtain the contact angle.

To extract the equilibrium contact angle from the image of the meniscus, we calculated the meniscus radius using a special Mallab based algorithm <sup>1</sup>. An example of the meniscus arc determination is shown in Fig. S2 b). **Table 2** collects the obtained contact angles. The error takes into account an uncertainty in the determination of the meniscus and wall contours.

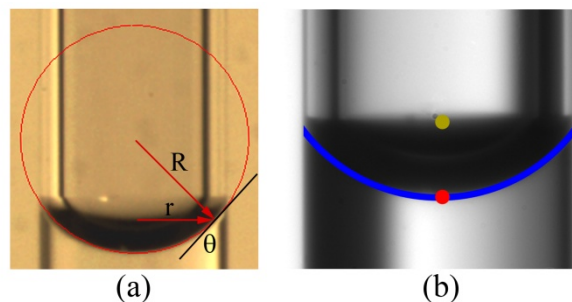


**Fig. S2** The best fit of the profile of equilibrium meniscus with a circle. Hexadecane in  $150\mu\text{m}$  radius capillary. Definition of the meniscus position using the upper and lower points of the shadow; these borders correspond to the upper and lower ends of the error bars.

These equilibrium contact angles were then checked using the meniscus tracking algorithm<sup>1</sup>, and solving Eq. (7). The procedure of the contact angle analysis was as follows. Analyzing the dynamics of meniscus advance at the short time intervals and using Eq. (6), we determined the friction coefficient in the capillaries of radii  $0.2\text{ mm} \leq R \leq 0.35\text{ mm}$ , **Figure S3**. Then using Eq.(7), we were able to fit the entire data set  $h(t)$  for hexadecane and for TBP using the contact angle as an adjustable parameter. Since the capillaries of smaller radii fall in the Regime II in Fig. 5 b), we used the obtained friction coefficient to fit the  $h(t)$  curve adjusting the contact angle. The results shown in Figure 4 confirm that the obtained friction coefficient and contact angle are correct. Then we averaged this set of data on contact angles and report the average contact angle for the given liquid, **Table 2**.

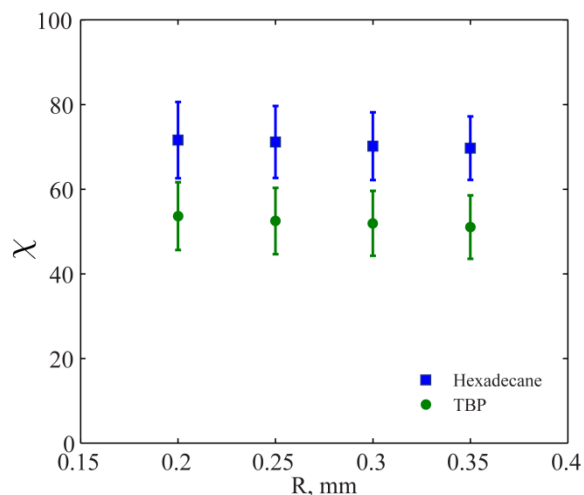


**Fig. S3.** Experimental friction coefficients measured on for different capillaries.

To confirm that these angles do characterize the liquid/glass pair and do not depend on any effects associated with gravity, we changed the capillary orientation from vertical to horizontal. The experiments were repeated with two sizes of capillaries with the inner radii of  $150\mu\text{m}$  and  $250\mu\text{m}$ . As an example, **Figure S4** shows the fitting results for the inner radius of  $150\mu\text{m}$ . The

contact angle  $\theta = 38^\circ$  provided the best fit of experimental data on vertical and horizontal capillaries of these two sizes. This contact angle lies within the experimental error specified in **Table 2**. Thus, the obtained contact angles summarized in **Table 2** provide a reliable set of data.

From comparison of the apparent dynamic contact angles and equilibrium contact angles, we conclude that the deviations are not very significant. Therefore, our model of linear friction of the contact line can be considered sufficient to describe the liquid uptake by capillaries.

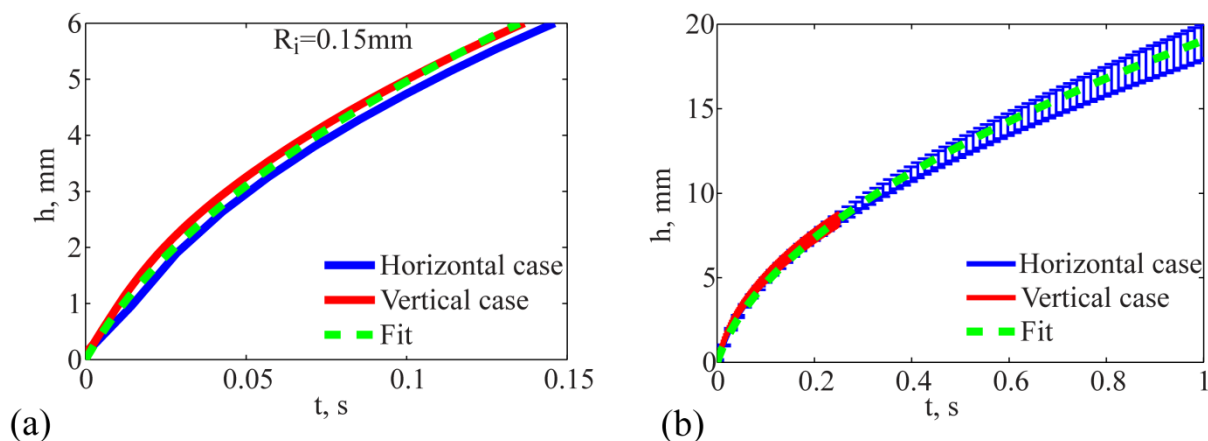


**Fig. S4.** **a)** Experimental data on uptake of hexadecane by capillary of  $150\mu\text{m}$  radius. The blue and red lines correspond to the experimental results on horizontal and vertical capillaries, respectively. The green dashed line is the best fit with the  $38^\circ$  contact angle. **b)** Continuation of the graph **a** to a longer time  $t$ . Observe that the green line representing the best fit of **a**) goes above all experimental points at longer time scale.

**Effect of air resistance.** To study the role of air resistance on the meniscus velocity, we have conducted experiments with 5 and 10cm long capillaries of  $200\mu\text{m}$  inner radius. Hexadecane was used in all experiments. Experiments revealed that the dynamics of the fluid uptake is practically the same for both cases, **Fig. S5**. Therefore we can safely neglect the air resistance.

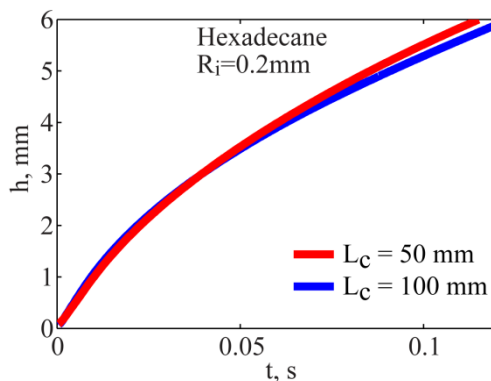


**Figure S5.** Meniscus position as a function of time in 5cm long capillaries (blue) and 10cm long capillaries (red).

### Effect of gravity.

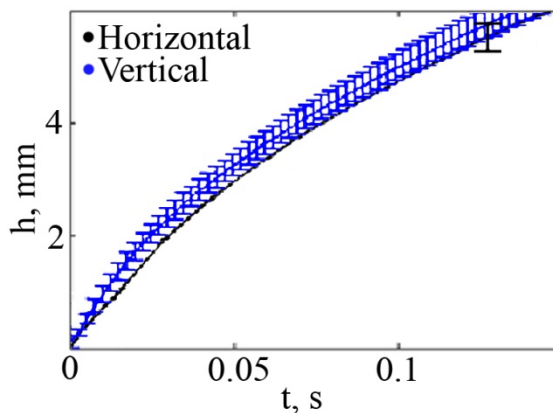


**Figure S6.** Position of hexadecane meniscus versus time. Vertical and horizontal configurations of the capillaries with 150 micrometer inner radius.

**Figure S6** shows an example of the data set for hexadecane meniscus moving through the 150  $\mu\text{m}$  capillaries held vertically and horizontally. As expected, no significant differences between the movements of menisci were observed within the time range in question. Therefore, one can safely assume that the gravity plays no significant role at the time scale where eq. (7) is applicable.

### References

1. T. Andruk, in *Materials Science & Engineering*, Clemson University, Clemson, 2012, p. 171.